molecular pharmaceutics

ARTICLE

pubs.acs.org/molecularpharmaceutics

Polyacrylamide Nanoparticles as a Delivery System in Photodynamic Therapy

Maheshika Kuruppuarachchi, Huguette Savoie, Ann Lowry, Cristina Alonso, and Ross W. Boyle*

Department of Chemistry, University of Hull, Cottingham Road, Kingston-upon-Hull, HU6 7RX, United Kingdom

ABSTRACT: Nanoparticles can be targeted towards, and accumulate in, tumor tissue by the enhanced permeability and retention effect, if sequestration by the reticuloendothelial system (RES) is avoided. The application of nanoparticles in the field of drug delivery is thus an area of great interest, due to their potential for delivering high payloads of drugs site selectively. One area which may prove to be particularly attractive is photodynamic therapy, as the reactive oxygen species (ROS) which cause damage to the tumor tissue are not generated until the drug is activated with light, minimizing generalized toxicity and giving a high degree of spatial control over the clinical effect. In the present study, we have synthesized two types of nanoparticles loaded with photodynamic sensitizers: polylysine bound tetrasulfonato-aluminum phthalocyanine entrapped nanoparticles (PCNP) and polylysine bound tetrasulfonato-aluminum phthalocyanine entrapped nanoparticles coated with a second, porphyrin based, photosensitizer (PCNP-P) to enhance the capacity for ROS generation, and hence therapeutic potential. The mean sizes of these particles were 45 ± 10 nm and 95 ± 10 nm respectively. Uptake of the nanoparticles by human Caucasian colon adenocarcinoma cells (HT29) was determined by flow cytometry and confocal microscopy. Cell viability assays using PCNP-P and PCNP corresponding to the minimum uptake time (<5 min) and maximum uptake time (25 h) demonstrated that these cancer cells can be damaged by light activation of these photodynamic nanoparticles both in the external media and after internalization. The results suggest that, in order to induce photodynamic damage, the nanoparticles need only to be associated with the tumor cell closely enough to deliver singlet oxygen: their internalization within target cells may not be necessary. Clinically, this could be of great importance as it may help to combat the known ability of many cancer cells to actively expel conventional anticancer drugs.

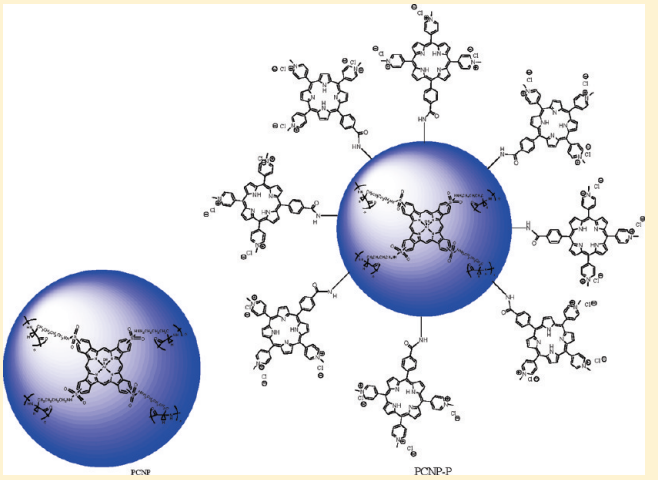

KEYWORDS: PDT, porphyrins, phthalocyanine, nanoparticles, drug delivery

1. INTRODUCTION

Photodynamic therapy (PDT) is a minimally invasive clinical procedure which holds great potential for treating many human diseases including several conditions of the skin, age related macular degradation and cancer.[1] PDT can be used alone or in combination with surgery, chemotherapy or ionizing radiation. PDT can also be used to destroy undetected cancerous cells at the margins of resection.[2] In advanced cancers, PDT gives the option of repeated treatments and allows clinicians to switch to more aggressive treatments, if needed. To induce tumor destruction, PDT requires three components: (i) a photosensitizer (PS) localized in the neoplastic tissue, (ii) light of a particular wavelength (to activate the PS), and (iii) oxygen. PSs are, in the context of PDT, compounds that absorb light of a specific wavelength and utilize that energy, in combination with molecular oxygen ($^3O_2$), to generate cytotoxic singlet oxygen ($^1O_2$).[3−6]

Various types of PSs have been synthesized in the last few decades,[3] and a few have been approved by drug administrations for use in the clinic.[7] However, some problems are associated with existing PSs,[8] including poor selectivity for tumor versus peritumoral tissue, and suboptimal photophysical characteristics. Hence, there is great interest in developing improved delivery systems. The ideal system should incorporate the PS without loss or alteration of PS activity and selectively accumulate the PS within the tumor tissue with little or no uptake by nontarget cells.[9]

Nanoparticles represent a relatively new trend in drug delivery.[10,11] Large particles (>200 nm) are usually captured by macrophages and typically exhibit a more rapid rate of clearance than particles with radii under 200 nm.[12] This can help to maintain higher circulating levels of the therapeutic agents once administered.[13] Drugs or biosensors can be entrapped in the nanoparticle matrix, conjugated to the nanoparticle surface or covalently linked to the nanoparticle matrix. There are advantages to entrapping drugs/sensors in the core of porous nanoparticles.[14] Primarily, the particle matrix acts as a barrier between the intracellular environment and potentially toxic dyes,

Received: January 17, 2011
Accepted: March 16, 2011
Revised: March 9, 2011
Published: March 16, 2011

Table 1. Type of Nanoparticles Synthesized

Type of Nanoparticles synthesised	
Non-functionalised, photosensitiser entrapped polyacrylamide nanoparticle	Polymer bound tetrasulfonato- aluminium phthalocyanine entrapped Nanoparticles (PCNP)
Polyacrylamide nanoparticles bound to two different photosensitisers (1. Entrapped in the matrix, 2. Conjugated to the surface)	Polymer bound tetrasulfonato-aluminium phthalocyanine entrapped, porphyrin conjugated nanoparticles (PCNP-P)

while inhibiting interactions between the dye and circulating serum components, which could potentially alter the dye's photophysical properties.

Endocytosis is one of the major pathways of nanoparticle cellular uptake,[15−17] and this process is both concentration and time dependent. Uptake of nanoparticles *via* endocytosis can occur through phagocytosis, fluid phase pinocytosis or receptor mediated endocytosis. Nanoparticles less than 200 nm are known to be imported into cells by pinocytosis while larger particles (>500 nm) are internalized through phagocytosis.[18] Panyam et al. reported no phagocytic activity with nanoparticles approximately 100 nm in size.[19]

Exocytosis is the reverse process to endocytosis in eukaryotic cells.[20] Endocytosis and exocytosis are both dynamic and energy dependent processes.[19] At any point in time, the nanoparticle concentration within a cell results from the net difference between these two processes. The intracellular population consists of nanoparticles that are recycling inside the cell, in the lysosomes, or in the cytoplasm.[19] Jin et al. reported a comparison of internalization (endocytotic uptake), exocytosis rates and net accumulation of carbon nano tubes over time (8000 s) compiled from single particle tracking and found that the net accumulation fluctuates with time.[21]

Nanoparticles used in drug delivery should be within the range 3−200 nm.[11] In targeting nanoparticles to tumor tissue, provided they can avoid sequestration by the reticuloendothelial system (RES), accumulation can occur in the stroma as a result of the enhanced permeability and retention effect.[22]

Particles synthesized to avoid the RES can lead to longer circulation times,[23] resulting in greater potential to reach the site of interest.[24] These nanoparticles were approximately 100 nm in size with a hydrophilic surface (to avoid clearance by fixed macrophages); this can be achieved by coating the particles with hydrophilic polymers that create a cloud of chains on the particle surface repelling plasma proteins.[22]

Polyacrylamide nanoparticles are hydrophilic and have demonstrated potential in drug delivery.[25] They have most commonly been used to monitor intracellular analytes (H^+, Ca^{2+}, Mg^{2+}, Zn^{2+}, O^{2-}, K^+, Na^+, Cl^-, OH, glucose)[14,26,27] and metabolites.[28] They have also been investigated as a delivery system for photosensitizers[29] with some successful results reported *in vivo*.[30,31]

In the present study, two types of polyacrylamide NPs (Table 1) are used to study the PDT activity in the human Caucasian colon adenocarcinoma cell line-HT29.

Physically entrapped dyes in polyacrylamide nanoparticles have previously been reported to leach 45−50% of their contents in 48 h[14,32] and up to 100% over seven days[32] when in an aqueous suspension. Factors such as the molecular size and hydrophilicity of the dye play a significant role in leaching properties of the dye from a polyacrylamide matrix.[32] Smaller dyes have a higher tendency to diffuse through the pores of the matrix. Further, hydrophobic dyes may have a tendency to stay near the surface of the particle matrix. To overcome leaching problems, nanoparticle pore size can be decreased by varying the type and the concentration of the cross-linker used in the nanoparticle synthesis,[32] covalently attaching the dye to the nanoparticle matrix;[33] or, by adding cages or lipophilic tails[27] to the dye. In this study, we have minimized/overcome the leaching of the entrapped photosensitizer by conjugating it to polylysine (MW 30,000−70,000).

Nanoparticles accumulate in the stroma of tumors due to selective retention.[34] To effect PDT, the nanoparticles need only to be associated with the tumor cell closely enough to deliver singlet oxygen and it may not be necessary that they are internalized within the target cells.[29] In order to investigate this hypothesis we have irradiated HT29 cells with nanoparticles present in the surrounding medium, at the time corresponding to minimum uptake time (<5 min), when <5% internalization has occurred as determined by flow cytometry. In order to compare these results with those of maximal uptake, we have conducted parallel experiments in which the same cells were incubated with particles for the time corresponding to maximal uptake (25 h), and irradiated after removing any particles remaining in the external media. In this way we hoped to mimic *in vivo* scenarios where particles have accumulated in the stroma surrounding the

cancer cells, but not penetrated them, and when particles have been internalized by endocytosis.

Common delivery methods for internalizing polyacrylamide nanoparticles into cells include liposomal delivery,[32,35] gene gun bombardment,[35,36] and picoinjection.[32,37,38] Further, specific targeting of polyacrylamide nanoparticles can be achieved by conjugating cell penetrating peptides to nanoparticles.[39] Ingestion of nanoparticles into a cell involves their attachment to the cell surface followed by internalization due to endocytosis.[19,40−42] Although ingestion of polyacrylamide nanoparticles has been reported,[37] as far as we are aware, this is the first attempt to qualitatively and quantitatively study polyacrylamide nanoparticle uptake (by endocytosis) to assess their potential as a delivery system for photodynamic sensitizers.

Nanoparticle uptake at regular intervals was quantified using flow cytometry. Confocal microscopy qualitatively confirmed nanoparticle internalization. Using this information, PDT induced cytotoxicity was quantified at times of minimal and maximum net uptake, in order to investigate the relative phototoxicity of the species when located in close proximity, but external to the cell, and internalized within the cell.

2. MATERIALS AND METHODS

Materials. AlPc-tetrasulfonic acid was purchased from Frontier Scientific. All the other reagents were purchased from Sigma Aldrich and used as received unless otherwise stated.

Methods. *Aluminum Phthalocyanine (AlPc) Tetrasulfonyl Chloride Synthesis.* AlPc-tetrasulfonic acid (200 mg, 0.23 mmol) and chlorosulfonic acid (0.8 mL) were stirred for 3 h at 100 °C. Thionyl chloride (1.2 mL) was added followed by stirring for 2 h at 80 °C. Once cooled to room temperature, the solution was poured onto ice and the AlPc-tetrasulfonyl chloride collected by centrifugation and filtration and dried *in vacuo* to obtain the product in 95% yield (0.22 g).

MW 30,000−70,000 Polylysine Conjugated Phthalocyanine (PC) Synthesis. AlPc-tetrasulfonyl chloride (100 mg, 0.1 mmol) was added, in small portions, to a solution of poly-D-lysine hydrobromide (MW 30,000−70,000) (50 mg, 0.4 mmol, 4 equiv) and sodium carbonate (85 mg, 0.8 mmol, 8 equiv) in water (4 mL), while vortexing for 1 min between each addition. Ten milliliters of the dispersion were dialyzed against PBS buffer using ultra membrane filters (MWCO 14 000) over 4 days to remove any unconjugated PC. MW 30,000−70,000 polylysine conjugated PC was collected and dried *in vacuo* in 95% yield (104 mg).

MW 30,000−70,000 Polylysine Conjugated PC Entrapped Polyacrylamide Nanoparticle Synthesis. Pc-polylysine NPs were synthesized by adopting the free radical microemulsion polymerization procedure optimized by Josefsen et al.[43] Briefly, a final volume of 1.9 mL containing acrylamide (540 mg, 7.60 mmol) and *N,N′*-methylenebisacrylamide (160 mg, 1.04 mmol) in water (1.7 mL) followed by a solution (100 μL) of Pc polylysine (1.34 mol dm^{-3}) was added to a deoxygenated hexane (42 mL) solution containing Brij 30 (3.08 g, 8.49 mmol) and completely dissolved dioctyl sulfosuccinate sodium salt (1.59 g, 3.58 mmol). A solution (30 μL, 0.4382 mol dm^{-3}) of ammonium persulfate (100 mg, 0.4382 mmol) in water (1 mL) followed by TEMED (15 μL, 0.1 μmol) was added, and the reaction was stirred for 2 h under a positive argon pressure at room temperature. Excess hexane was removed *in vacuo*. The resulting viscous yellow colored solid was washed with ethanol, centrifuged (8 × 50 mL, 10 min, 4500 rpm) and recovered by microfiltration (Whatman Anodisc 25, 0.02 μm, 25 mm filters) to yield the desired Pc polylysine entrapped nanoparticles. Yield: 86% (602 mg).

MW 30,000−70,000 Polylysine Conjugated AlPc Entrapped Amino Functionalized Polyacrylamide Nanoparticle Synthesis. To synthesize amino functionalized nanoparticles, the above nanoparticle synthesis procedure was followed with the exception of addition of *N*-(3-aminopropyl)methacrylamide hydrochloride (1% equivalence to acrylamide) along with the monomers. Briefly, a final volume of 1.900 mL containing acrylamide (527 mg, 7.41 mmol), *N,N′*-methylenebisacrylamide (160 mg, 1.04 mmol) and *N*-(3-aminopropyl)methacrylamide hydrochloride (13 mg, 0.073 mmol) in water (1.7 mL) followed by a solution 100 μL of Pc polylysine (1.34 mol dm^{-3}) was added to a deoxygenated hexane (42 mL) solution containing Brij 30 (3.08 g, 8.49 mmol) and completely dissolved dioctyl sulfosuccinate sodium salt (1.59 g, 3.58 mmol). A solution (30 μL, 0.4382 mol dm^{-3}) of ammonium persulfate (100 mg, 0.4382 mmol) in water (1 mL) followed by TEMED (15 μL, 0.1 μmol) was added, and the reaction was stirred for 2 h under a positive argon pressure at room temperature. Excess hexane was removed *in vacuo*. The resulting viscous yellow colored solid was washed with ethanol, centrifuged (8 × 50 mL, 10 min, 4500 rpm) and recovered by microfiltration (Whatman Anodisc 25, 0.02 μm, 25 mm filters) to yield the desired Pc polylysine entrapped nanoparticles. Yield: 88% (616 mg).

5-(4-Carboxyphenyl)-10,15,20-tri-(4-pyridyl)porphyrin.[44] Dropwise, pyrrole (4 mL, 57.8 mmol) was added to a refluxing mixture of 4-formylbenzoic acid (2.54 g, 17 mmol) and 4-pyridinecarboxaldehyde (9.78 mL, 104 mmol) in acetic acid (200 mL) and nitrobenzene (150 mL). The reaction mixture was kept under reflux and intense stirring for 1 h. The solvents were removed under reduced pressure, and the residue was purified by column chromatography using a mixture of 15% dichloromethane/methanol as an eluent system. Pure 5-(4-carboxyphenyl)-10,15,20-tri-(4-pyridyl)porphyrin was obtained after precipitation from methanol over chloroform in 6% in yield (510 mg).

5-[4-(Succinimide-N-oxycarbonyl)phenyl]-10,15,20-tri-(4-pyridyl)porphyrin[45]. To a stirred solution of 5-(4-carboxyphenyl)-10,15,20-tri-(4-pyridyl)porphyrin (51.1 mg, 0.077 mmol) in dry pyridine (5 mL) was slowly added thionyl chloride (0.1 mL, 1.37 mmol, 18 equiv). The reaction was stirred at 50 °C, protected from light and atmospheric moisture, for 30 min. *N*-Hydroxysuccinimide (200 mg, 1.74 mmol, 22.6 equiv) was then added, and the mixture was kept stirring under the previous conditions for a further 3 h. Pyridine was then removed under vacuum and the residue taken up in dichloromethane and washed with an aqueous saturated solution of sodium carbonate. The organic layer was dried over sodium sulfate and evaporated to dryness under reduced pressure. Crystallization of the residue in light petroleum over chloroform afforded pure 5-[4-(succinimide-*N*-oxycarbonyl)phenyl]-10,15,20-tri-(4-pyridyl) porphyrin in 90% yield (52.3 mg). ^{1}H NMR ($CDCl_3$, 400 MHz) δ: −2.90 (br s, 2H, NH), 3.03 (br s, 4H, CH2), 8.17 (dd, 6H, 10,15,20-H-Ar-*o*, J 1.6, 4.3 Hz), 8.37 (dd, 2H, 5-H-Ar-*m*, J 1.7, 6.5 Hz), 8.57 (dd, 2H, 5-H-Ar-*o*, J 1.7, 6.5 Hz), 8.85 (d, 2H, H-β, J 4.8 Hz), 8.86−8.90 (m, 6H, H-β), 9.06 (dd, 6H, 10,15,20-H-Ar-*m*, J 1.6, 4.3 Hz). ^{13}C NMR ($CDCl_3$, 400 MHz) δ: δ: 25.8, 30.0 (CH2), 117.8, 129.1, 129.3 (10,15,20-Ar-*o*-C), 134.8, 148.4 (10, 15,20-Ar-*m*-C),149.8, 150.2, 162.0 (CO2N), 169.3 (CON). Mass (MALDI): *m*/*z* 759. UV−vis: 420, 519, 555, 580, 636 nm.

5-[4-(Succinimide-N-oxycarbonyl)phenyl]-10,15,20-tris-(4-N-methylpyridimiumyl)porphyrin Triiodide[45]. To a stirred solution of 5-[4-(succinimide-*N*-oxycarbonyl)phenyl]-10,15,20-tri-(4-pyridyl)porphyrin (26 mg, 0.0343 mmol) in dry DMF (5 mL) was added a large excess of methyl iodide (0.5 mL, 8.03 mmol) *via* syringe. The reaction mixture was kept stirring at 40 °C, under a nitrogen atmosphere and protected from light overnight. The product was then precipitated with diethyl ether to remove any trace of methyl iodide and DMF. The resulting solid was filtered and dissolved in acetone/water (50:50), and the solvents were removed under reduced pressure. Pure 5-[4-(succinimide-*N*-oxycarbonyl)phenyl]-10,15,20-tris-(4-*N*-methylpyridimiumyl)porphyrin triiodide was obtained after a new precipitation in acetone over water in 89% yield (31.6 mg). ^{1}H NMR ($CDCl_3$, 400 MHz) δ: −3.05 (br s, 2H, NH), 3.01 (br s, 4H, CH2), 4.71 and 4.72 (2s, 6 + 3H, CH3), 8.50 (d, 2H, 5-H-Ar-*m*, J 8.3 Hz), 8.60 (d, 2H, 5-H-Ar-*o*, J 8.3 Hz), 9.00 (d, 6H, 10,15,20-H-Ar-*o*, J 6.6 Hz), 9.04−9.13 and 9.14−9.22 (2 m, 8H, H-β), 9.48 (d, 6H, 10,15,20-H-Ar-*m*, J 6.6 Hz). Mass (MALDI): *m*/*z* 804. UV−vis: 420, 520, 554, 582, 635 nm.

5-[4-(Succinimide-N-oxycarbonyl)phenyl]-10,15,20-tris-(4-N-methylpyridimiumyl)porphyrin Trichloride. To a solution of 5-[4-(succinimide-*N*-oxycarbonyl)phenyl]-10,15,20-tris-(4-*N*-methylpyridimiumyl)porphyrin triiodide (56.9 mg, 0.0481 mmol) in anhydrous methanol (57 mL) was added Dowex 1×8 200−400 Cl (1.81 g), and the reaction mixture was stirred at room temperature for 1 h, protected from moisture and light. The resin was separated by filtration and the reaction mixture concentrated under reduced pressure. After precipitation with acetone, pure 5-[4-(succinimide-*N*-oxycarbonyl)phenyl]-10,15,20-tris-(4-*N*-methylpyridimiumyl)porphyrin trichloride was obtained as a brown solid in 96% yield (41.8 mg). ^{1}H NMR (DMSO-d_6, 400 MHz) δ: −3.05 (br s, 2H, NH), 3.01 (br s, 4H, CH2), 4.72 and 4.73 (2s, 6 + 3H, CH3), 8.50 (d, 2H, 5-H-Ar-*m*, J 8.0 Hz), 8.60 (d, 2H, 5-H-Ar-*o*, J 8.0 Hz), 9.00 (d, 6H, 10,15,20-H-Ar-*o*, J 5.6 Hz), 9.05−9.12 and 9.13−9.24 (2 m, 8H, H-β), 9.49 (d, 6H, 10,15,20-H-Ar-*m*, J 5.6 Hz). ^{13}C NMR (DMSO-d6, 100 MHz) δ: 25.7 (CH2), 47.9 (CH3), 115.0, 115.5, 120.7, 124.6, 128.9, 132.1 (10,15,20-Ar-*o*-C), 135.1, 144.2 (10,15,20-Ar-*m*-C), 147.3, 156.4, 162.0 (CO_2N), 170.5 (CON). Mass (MALDI): *m*/*z* 804. UV−vis: 421, 519, 554, 584, 637 nm.

Conjugation of 5-[4-(Succinimide-N-oxycarbonyl)phenyl]-10,15,20-tris-(4-N-methylpyridimiumyl)porphyrin Trichloride to Polyacrylamide Nanoparticles. An aliquot of (500 μL, 2.2 mmol dm^{-3}) of succinimide-*N*-oxycarbonyl)phenyl]-10,15,20-tri(4-*N*-methylpyridiniumyl porphyrin was added to a dispersion (10 mL) of filtered (Millex GP, 0.22 μm Filter unit) amino functionalized AlPc-polylysine entrapped nanoparticles (50 mg) and triethylamine (250 μL). The mixture was spun in Falcon polystyrene (12 × 75 mm) tubes for 2 h on a spinning rotator at room temperature, protected from light. The resulting suspension was washed with ethanol, centrifuged (7 × 50 mL, 10 min, 5500 rpm), microfiltered (Whatman Anodisc 25, 0.02 μm, 25 mm filters) and dried for 8 h at 40 °C to yield the desired porphyrin conjugated PC entrapped nanoparticles as a green solid. Yield: 78% (39 mg).

Characterization of Nanoparticles. *Particle Size.* The particle size and size distribution properties of the nanoparticles were measured by PCS, Zetaplus particle size analyzer (Malvern 3000) at 25 °C and at a scattering angle of 90°. A dilute sample of nanoparticles (1 mg/mL) was prepared in Milli-Q water, sonicated for 30s and filtered (Millex GP, 0.22 μm filter unit) before analysis. The value was recorded as the average of 30 data measurements.

TEM Imaging. The nanoparticles were suspended in deionized water and placed in an ultrasonic bath for 3 min. The suspension was then passed through a Millex GP, 0.22 μm filter unit and the resulting suspension returned to the ultrasonic bath for a further 2 min to disperse any aggregates. Five microliters of the suspension was immediately put onto a hydrophilic carbon coated copper grid (Agar Scientific Ltd., Stansted, Essex, U.K.) and allowed to air-dry. Dry ethanol (5 μL) was then added to the grid and left to air-dry. TEM images were obtained using an UltraScan 4000 digital camera (Gatan UK, Abingdon) attached to a Jeol 2010 transmission electron microscope (Jeol (UK) Ltd. Welwyn Garden City) running at 120 kV.

Determination of the Entrapped Phthalocyanine (PC) Concentration and the Conjugated Photosensitizer Concentration. One milligram of filtered (Millex GP, 0.22 μm filter unit) nanoparticles was dispersed in 1 mL of deionized water and the absorbance of the particles measured by UV spectrophotometry (Varian Cary50 Bio; Cary WinUV) between the wavelengths 400 and 800 nm.

The concentrations of the entrapped Pc and Porphyrin concentration were quantified using the Beer−Lambert law ($A = \varepsilon CL$; *A*, absorbance; ε, extinction coefficient of the compound; *C*, concentration; *L*, path length). The reported extinction coefficient for Al-Pc calculated from absorbance at 666 nm is 1.5×10^5 M^{-1} cm^{-1}, and the measured extinction coefficient for NHS porphyrin calculated from absorbance at 520 nm is 2.3×10^5 M^{-1} cm^{-1}.

Leaching of Entrapped PC Polylysine from the Nanoparticles. Leaching of the PC-polylysine from the nanoparticles was studied to assess the porosity of the nanoparticles. Nanoparticles (200 mg) were dispersed in 80 mL of Milli-Q water. The dispersion was kept stirring at room temperature. At given time intervals (hourly), three 2 mL samples were drawn from the suspension and the nanoparticles were microfiltered (Whatman Anodisc 25, 0.02 μm, 25 mm filter). The filtrate was analyzed by fluorescence microscopy.

Determination of Singlet Oxygen Production. Two milliliters of DCM followed by 3 mL of cholesterol 10 mM (1:9 DCM:MeOH) was added to a nanoparticle (5 mg/1 mL MeOH) suspension. Oxygen was bubbled through the resulting suspension mixture, which was then irradiated with white light (400−700 nm) for one hour. The mixture volume was reduced to dryness by flowing argon into the suspension. One milliliter of MeOH was added, and the suspension was filtered through a 15 nm filter (Whatman Nuclepore track-etched membrane; 25 mm, 0.015 μm). 200 μL of this solution was transferred to an Eppendorf (tube), and 200 μL of methanol was added. 1−2 crystals of $NaBH_4$ were added to the solution, which was left for 1 min until complete reduction had taken place. The volume of the solvent was reduced to approximately 100−150 μL by flowing argon over the solution.

TLC plate development was carried out using the method described by van Lier et al.[46] Briefly, a TLC plate was placed in a tank containing 1:1 hexane:ethyl acetate mixture. The solvent was allowed to migrate 2/3 of the way up the plate; the plate was then removed from the TLC chamber and allowed to air-dry. Once dried, the plate was returned to the tank and the solvent was allowed to migrate to the top of the plate and was left dry again. To visualize the sterols on the TLC plate, a 5% H_2SO_4 in

ethanol mist was sprayed onto the TLC plate and the plate placed on a 100−120 °C hot plate to allow development of the colored spots.

The HPLC method for quantifying the singlet oxygen production was adopted from Osada et al.[47] Cholesterol and its oxidative derivatives were separated on a Phenomenex Luna 5 μm C18 column (250 × 4.60 mm) using a mixture of methanol:acetonitrile (60:40 vol/vol) mobile phase. The flow rate was maintained at 1.0 mL/min for 20 min prior to analysis. UV detection was performed at 205 nm. Ten microliters of the sample was injected manually into the HPLC analysis system, and the separation was detected using the Azur software.

Cell Line Experiments. *Cell Culture.* HT29 cells were routinely cultured in 75 cm^3 tissue culture flasks in McCoy's 5A medium supplemented with 10% fetal calf serum (FCS), 1% L-glutamine (all purchased from PAA) at 37 °C in a humidified environment of 5% CO_2. The medium was replenished every day, and the cells were subcultured after reaching confluence. PBS, BSA, and sodium azide were purchased from Sigma Aldrich, U.K.

Cellular Uptake (FACS) of Nanoparticles. The cell uptake of PCNP nanoparticles was studied using HT29. This cell line was selected due to the large amount of data published on PDT effects of photosensitizers using these cells.

A time course experiment was carried out by setting up a control (cells only) and 2 samples (cells and nanoparticles) at each given time point. Cell-only controls contained 50,000 cells in 400 μL of McCoy's high glucose medium, and each sample contained 50,000 HT29 cells and 10 mg of polylysine conjugated phthalocyanine entrapped nanoparticles in 400 μL of medium (10 mg of nanoparticle suspension in 200 μL of medium was added to a sterile Falcon polystyrene (12 × 75 mm) tube containing 50,000 cells in 200 μL of medium).

Both the control and sample systems were incubated at 37 °C, in an atmosphere of 5% CO_2 within a humidified incubator. At given time points, duplicate sample tubes and a control tube were taken out of the incubator, washed, and resuspended in ice cold PBS/BSA/azide solution before preparation of the material for flow cytometry.

Following incubation, 4 mL of the PBS/BSA/azide solution was added to all three tubes, and the cells were pelleted by centrifugation at 404*g* for 5 min. The supernatant was removed and discarded, and the cells were resuspended in 1 mL of PBS/BSA/azide solution and transferred to a clean tube. The cells were washed again by adding a further 3 mL of PBS/BSA/azide. The cells were pelleted once again by centrifugation at 404*g* for 5 min. The washing procedure was repeated twice more, before the cells were resuspended in 200 μL of PBS/BSA/azide solution.

The cell suspension was loaded into a hemocytometer after 5 min to count the cells. Results were then acquired using a Becton Dickinson FACS Calibur flow cytometer with the following settings: forward scatter (FSC) E −1 752, side scatter (SSC) 369; fluorescence (FL1) log 412; fluorescence (FL2) log 474, fluorescence (FL3) log 427, fluorescence (FL4) log 377. A minimum of 10,000 cells was measured in each sample.

PCNP were detected in the fluorescence level (FL4) channel of the flow cytometer. Analysis was performed using CellQuest Pro V software (Becton Dickinson), and histograms were plotted of FL4 fluorescence versus cell counts for each time point. The cell-only sample provided the negative control at each time point.

Chart 1. PCNP Absorbance and Emission Spectra

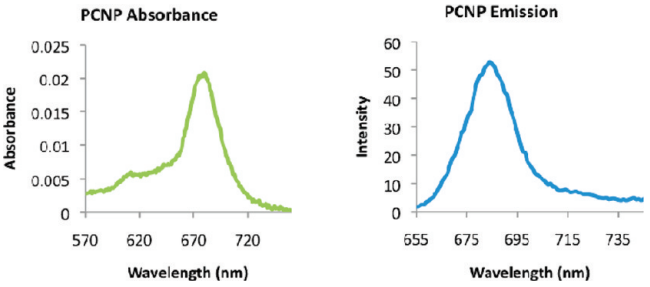

Photocytotoxicity: In Vitro HT 29 Cells (Maximum Uptake). Ten milligrams of nanoparticles was added to 1 mL of McCoy's medium, vortexed (60 s), sonicated (60 s) and filtered (Millex GP, 0.22 μm filter unit). The obtained volume (approximately 800 μL) was added to the same volume of cells (2.5 × 10^5 cells/1 mL) in a Falcon polystyrene (12 × 75 mm) tube. The tube was incubated for 25 h at 37 °C in a humidified environment of 5% CO_2. The volume of the medium was increased to 4 mL, and after centrifugation, the supernatant was discarded to eliminate any interference from nanoparticle conjugates that had not been internalized or attached to the HT29 cells. The volume of medium was increased to the initial volume (approximately 800 μL). HT29 cells were plated with 100 μL of cell suspension per well in two 96 well plates. The two controls, cells only (100% cell survival) and medium only (background control) were plated onto each plate.

One plate was irradiated with 7 J/cm^2 [~23 min] followed by a 40 min recovery period in the incubator (at 37 °C in a humidified environment of 5% CO_2) and another 7 J/cm^2 using an Oriel light system (>580 nm red schott glass filter, 51310/59510). The second plate was kept in the dark outside the incubator while the other plate was being irradiated. The plates were left to incubate overnight for 18−24 h in the dark. To determine cell viability, the colorimetric MTT (3-[4, 5-dimethylthiazol-2-yl]-2,5-diphenyltetrazolium bromide; Sigma Aldrich) metabolic activity assay developed by Mossman,[48] and subsequently modified by Prasad and co-workers to incorporate a cell irradiation protocol,[49] was used. The cell viability was determined using a microplate reader (BioTek EL 800).

Photocytotoxicity: In Vitro Photodynamic Therapy Experiments with HT 29 Cells (Minimum Uptake). Nanoparticles and cells were prepared and plated as above and without incubating the cells with nanoparticles or washing prior to irradiation. The light control plate was irradiated with the same system described above soon after plating (<5 min) 7 J/cm^2 [~23 min] followed by a 40 min recovery period in the incubator (at 37 °C in a humidified environment of 5% CO_2) and another 7 J/cm^2. Meanwhile the dark control plate was kept outside the incubator in the dark. The controls, cells only (100% cell survival) and medium only (background control), were each plated in a 96 well plate.

The wells were washed with 3 × 100 μL of medium. 100 μL of medium was added to the wells, and the plates were left to incubate overnight for 18−24 h in the dark. MTT activity assays were used as above to determine cell viability.

Fluorescence Confocal Microscopy. One milliliter of PCNP (10 mg/mL) and PCNP-P (10 mg/mL) was added to separate Falcon polystyrene (12 × 75 mm) tubes containing 1 mL (2.5 × 10^5/mL) of HT29. These were incubated for 20 h at 37 °C in a

humidified environment of 5% CO_2 and washed three times with McCoy's medium.

The intracellular localization of the nanoparticles was observed with a Leica Microsystems CMS Gmbh (LAS AF version: 2.2.1 build 4842). To observe the PCNP the incubated cells with PCNP were excited at 633 nm and the emission was collected between 648 and 790 nm. Similarly, PCNP-P localization was observed by exciting the incubated cells with PCNP-P at 405 nm and 633 nm and emission collected between 420 and 790 nm and between 648 and 794 nm respectively.

3. RESULTS AND DISCUSSION

Nanoparticle Synthesis and Characterization. PC-polylysine (MW 30,000−70,000) entrapped polyacrylamide nanoparticles were synthesized by adopting the well documented microemulsion polymerization method used in previous work from this laboratory[43] and others.[37] The polylysine was conjugated to PC to minimize leaching once entrapped in the polyacrylamide matrix. The absorbance and emission spectra confirmed that the PC is entrapped intact within the nanoparticle matrix (Chart 1).

It should be noted that all the nanoparticle suspensions were prepared in deionized water and filtered through a Millex GP, 0.22 μm filter unit prior to any preliminary characterizations or secondary experiments unless stated otherwise.

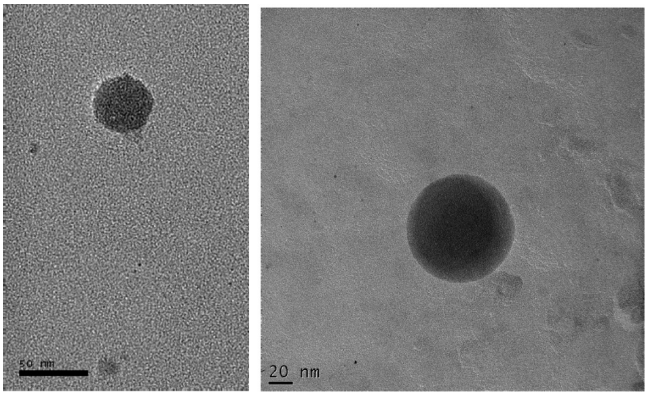

Figure 1. TEM - PCNP, PCNP-P.

The mean particle size, 45 (±10 nm), was determined by PCS and TEM images (TEM, Figure 1). Amino functionalization of the PCNP-A was confirmed using a fluoroscamine test.[50]

Leaching of the PCNP was studied using fluorescence spectroscopy. This technique was used due to its high sensitivity (approximately 1000 times more than absorption spectroscopy). In the experiment, hourly, three 2 mL aliquots were drawn from the suspension (200 mg of nanoparticles in 80 mL of Milli-Q water), the nanoparticles were microfiltered and the supernatant was analyzed by fluorescence microscopy. Maximum leaching of the PC from the nanoparticles peaked at 3 h (Chart 2), and the level of fluorescence remained at the same level. This may suggest that the majority of loosely trapped PC molecules are "removed" from the nanoparticle suspension within this time. The fluorescence intensity of the filtrate dropped slowly between 3 and 24 h. Thus, it can be hypothesized that no further leaching occurred after the first three hours. The slight drop in the fluorescence level of the filtrate after three hours could be due to photobleaching due to the much smaller concentration of fluorescent material (PC) in the filtrate. Amino functionalized PCNP offered a similar observation.

To synthesize the PCNP-P, PCNP-A (in suspension) was mixed with synthetic porphyrin engineered to bear a single amine-reactive succinimide-*N*-oxycarbonyl-phenyl group in water for one hour. The nanoparticles were then precipitated and washed (5 times, 50 mL) with ethanol.

Successful conjugation of 5-[4-(succinimide-*N*-oxycarbonyl)-phenyl]-10,15,20-tri(4-*N*-methylpyridiniumyl porphyrin) to PCNP-A was confirmed by clear absorbance peaks at 424 nm (porphyrin, Soret band) and 680 nm (PC, Q-band) respectively. When excited at 424 nm, the PCNP-P emission spectrum showed two clear fluorescence peaks (656 and 708 nm) corresponding to the porphyrin and a minor peak relative to PC at 685 nm. However, when excited at 650 nm (close to the PC λ_{max} of 680 nm), a clear emission peak relating to the PC at 685 nm was observed (Chart 3).

As confirmed by the PCS and TEM images, the mean size of the PCNP-P was 95 ± 10 nm (Figure 1). The size of a porphyrin molecule is 18 Å, and thus the maximum size increase that was expected was ∼36 Å. Experiments were carried out to study the reasons for this unexpected increase in size of PCNP-A after conjugation to the porphyrin molecule.

One hypothesis was that the increase in the mean particle size upon porphyrin conjugation to PCNPs could be a result of

Chart 2. Leached Fluorescence over Time: Phthalocyanine Conjugated Polylysine (MW 30,000−70,000) Entrapped Nanoparticles

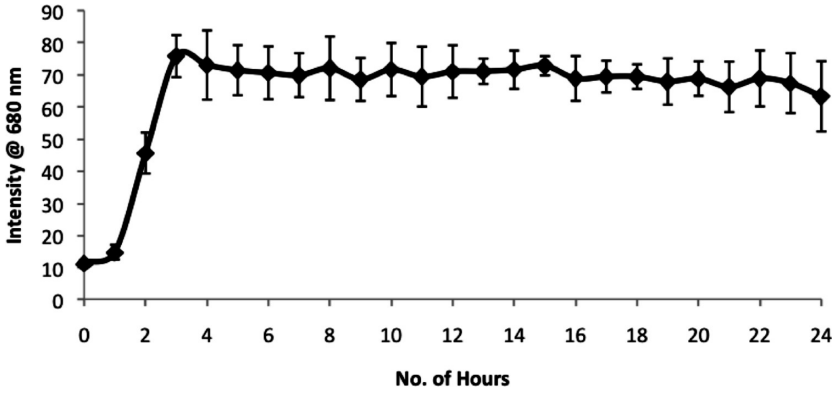

Chart 3. PCNP-P Absorbance and Emission Spectra

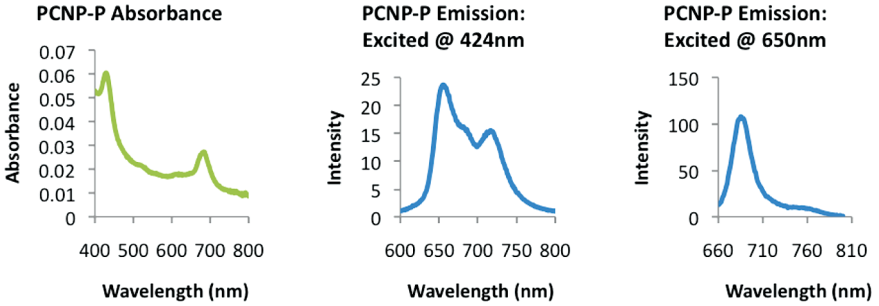

Chart 4. Fluorescence Spectrum of 5,10,15,20-Tetrakis(4-*N*-methylpyridyl)porphyrin[a]

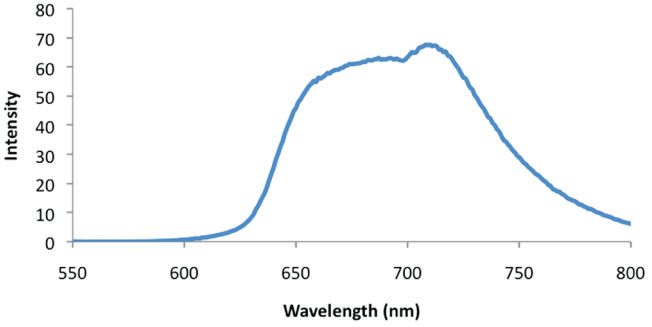

[a]NHS porphyrin emission (Ex: 424 nm).

Chart 5. PCNP-A and PCNP-P Absorbance Spectra Comparison[a]

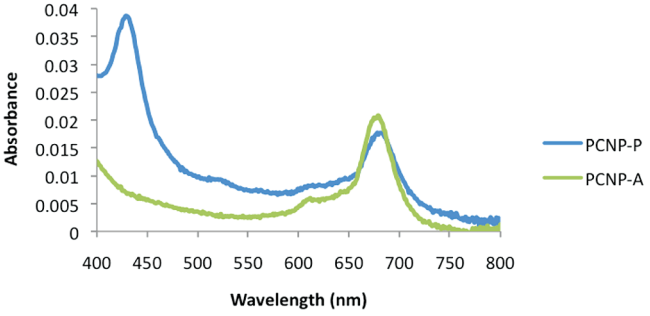

[a]1 mg of NPs; in 3 mL of water.

aggregation caused by porphyrin interactions on adjacent particles. This type of $\pi-\pi$ interaction could be detected in the fluorescence spectra of the NHS porphyrin used for conjugation, and is similar to the split fluorescence peaks reported for these interactions with the related 5,10,15,20-tetrakis(4-*N*-methylpyridyl)porphyrin[51](Chart 4).

Polyacrylamide hydrogels/nanogels are known to swell in aqueous environments.[52] Thus, an alternative hypothesis was that this effect was due to polyacrylamide swelling. In water, the swelling is controlled by several factors: the cross-linker concentration, pH and ionic strength.[52,53] However, experiments carried out to study whether the diameter increase was a result of this swelling behavior indicated that these parameters were not involved.

Leaching studies carried out with the PCNP-P showed no filtrate fluorescence; two photosensitizers (PC and porphyrin) were successfully conjugated to a polyacrylamide nanoparticle system (without leaching).

Absorbance spectra for one milligram of each PCNP-P and PCNP-A were compared to observe any differences in the PC concentration. The Q-band of PCNP-P showed a slight decrease (15−20%) of intensity compared to PCNP-A (Chart 5).

This could be either because any loosely entrapped PC was washed away during the conjugation procedure and/or the mass added by the conjugated porphyrin in the total weighed sample. The porphyrin−nanoparticle conjugation procedure generally takes approximately 3 h, and PC leached only in the first 3 h. During the conjugation procedure, it is possible that any loosely entrapped PC was washed away, leaving only the tightly entrapped PC in the nanoparticle.

The concentrations of the entrapped PC and porphyrin were quantified using the Beer−Lambert law: 1.9×10^{-4} M with respect to PC for PCNP-A and 1.6×10^{-4} M mol of PC and 1.8×10^{-4} M for PC and porphyrin, respectively, for PCNP-P. The drug loading of the batches reproduced using the stated concentrated was within standard deviation 5.09×10^{-8} (within 30%).

Nanoparticle Uptake. We have found that polyacrylamide nanoparticles do accumulate in cells, provided they are incubated with cells for a sufficient time period. Following this, we studied the fluctuation of the nanoparticle net uptake by flow cytometry over 28 h using PCNP with HT29 cells incubated at 37 °C in a humidified environment of 5% CO_2 (Chart 6). At every hour for the duration of the experiment, duplicate sample tubes and a control tube were taken out of the incubator, washed and resuspended in ice cold PBS/BSA/azide solution before preparation for flow cytometry.

Since both endocytosis and exocytosis are energy dependent functions,[17] ice cold washing steps were considered to have a minimal[54] and/or constant effect on nanoparticle uptake study. Further, it should be noted that the HT29 cell line used in the experiment naturally divides with time effectively reducing the quantity of nanoparticles in each cell by a factor of 2 with each division,[32] which could potentially have an impact on the internalization studies. Two concentrations (3 mg/mL and 5 mg/mL) of nanoparticles were studied, and the percentage

Chart 6. PCNP Net Uptake with HT29 over Time

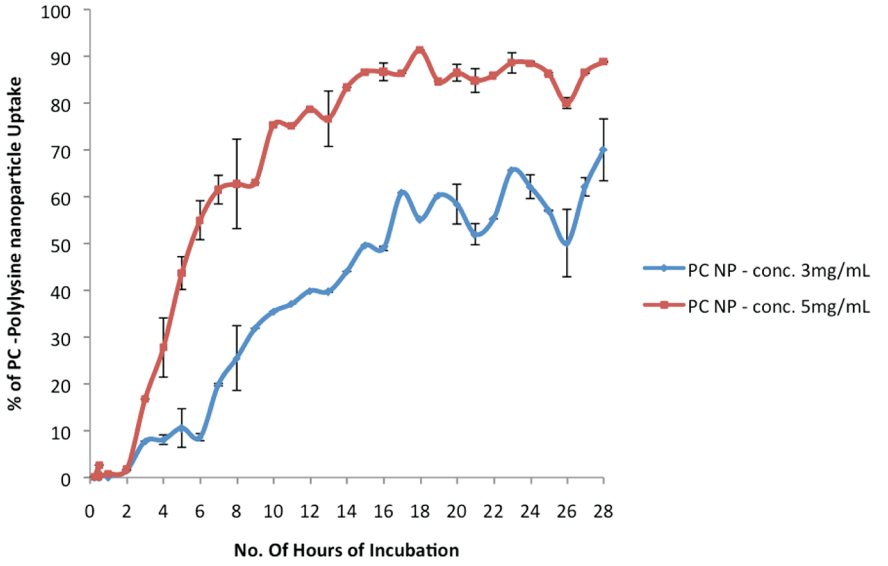

Chart 7. PCNP, PC NP (Amino), PC Porphyrin NP: Net Uptake with HT29 over Time

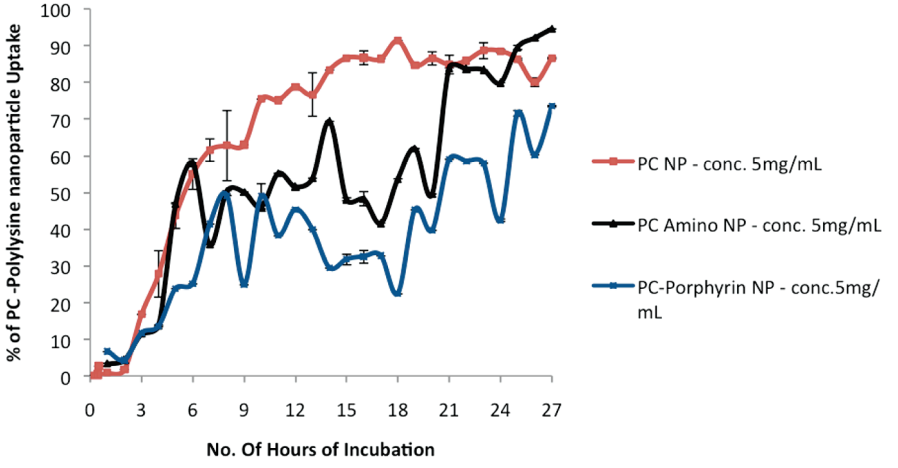

uptake values confirmed that nanoparticle uptake by HT29 was concentration dependent (Chart 6).

According to the quantified NP uptake profile, NP uptake reaches its maximum in 18 h and then remains constant, but with regular fluctuations. Alberola et al. showed a similar oscillation pattern in uptake of nanoparticles by epithelial cells using fluorescence microscopy.[55]

The same concentration (5 mg/1 mL) of both PCNP-A and PCNP-P demonstrated a similar, but more intense, fluctuation pattern as for PCNP (Chart 7).

All three nanoparticle types showed a relatively high uptake at 25 h. Thus, in the PDT cytotoxicity assays, cells were incubated with nanoparticles for 25 h before irradiation.

The cytotoxic agent in PDT is singlet oxygen. TLC (qualitatively) and HPLC (quantitatively) confirmed the singlet oxygen production by both NP types. PCNP-P produced 20% more singlet oxygen in comparison to PCNP.

PDT: Cytotoxicity Assays. Nanoparticles suspended in McCoys 5A medium were filtered through a 220 nm filter prior to any PDT cytotoxicity experiments as a sterilizing step. In cytotoxicity assays, generally ethanol is used to sterilize particles prior to incubation with cells. However, it is known that ethanol has the potential to disrupt the cell membranes even when present in small quantities,[56] and in the study, it was found that this caused unpredicted cell toxicity when incubating for longer periods, therefore its use was avoided.

The filtered high intensity (1000 W) quartz−tungsten halogen light system (>580 nm red SCHOTT glass filter, 51310/59510) with water cooling was used to compare the PDT activity of PCNP and PCNP-P. NPs were incubated for 25 h with HT29, and the cells were irradiated with 7 J/cm^2 [∼23 min] followed by 40 min recovery period in the incubator and another 7 J/cm^2 irradiation. The light dose (14 J/cm^2) was fractionated with a 40 min recovery period to allow reoxygenation of the media. The plates were left in the incubator overnight for 18−24 h in the dark. MTT activity assays were then used to determine the cell viability.

dx.doi.org/10.1021/mp200023y |*Mol. Pharmaceutics* 2011, 8, 920–931

Chart 8. PCNP and PCNP-P: PDT Cytotoxicity (Maximum Uptake)[a]

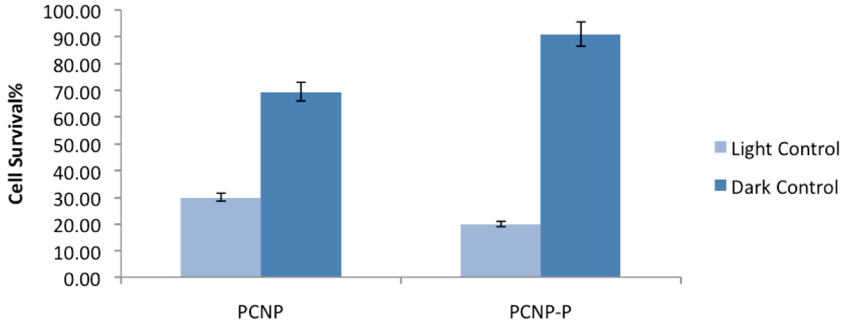

[a]25 h incubation; irradiation, 14 J cm^{-2}.

Chart 9. PCNP and PCNP-P: PDT Cytotoxicity (Minimum Uptake)[a]

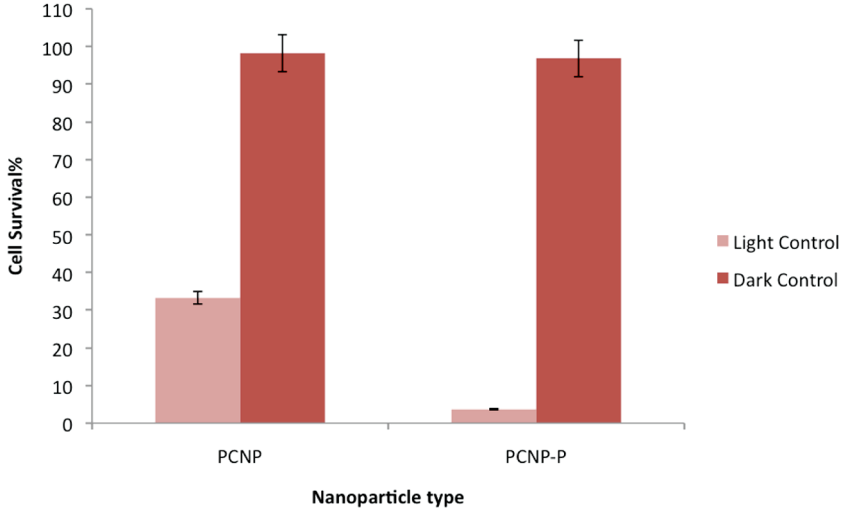

[a]0 h incubation; irradiation, 14 J cm^{-2}.

After irradiation cell viability of PCNP-P was 20% while the nonirradiated dark control was 91%. Cell viability of the PCNP following irradiation was 30% and the dark control was 70% (Chart 8).

Russell et al.[57] reported cell viability, after irradiation, of 43% and viability of 77% for an analogous experiment without irradiation with gold nanoparticles coated on the surface with phthalocyanines (diameter 2−4 nm). In this case, HeLa cells were incubated with the nanoparticles for 4 h, and irradiated with light at 690 nm (1.84 mW cm^{-2}) for 20 min.

Nanoparticles are reported to accumulate in tumor neovasculature due to selective retention.[34] Exploiting this notion *in vitro*, HT29 cells surrounded with nanoparticles, in the extracellular media, and at the minimum uptake time (<5 min) were irradiated under identical conditions to those used for the 25 h uptake time. MTT assays were then performed as before and cell viabilities determined (Chart 9).

PCNP-P showed the lowest cell viability post irradiation with only 3.7% of cells surviving, whereas the cell viability of PCNP was 33%. However, no noticeable dark toxicity was observed with either PCNP or PCNP-P. This result could be due to, in this instance, the nanoparticles being mixed with cells only for the duration of the irradiation (approximately 90 min).

These results are potentially very interesting from a clinical perspective, as it is likely that a significant proportion of nanoparticles would accumulate in the stroma of the tumor i.e. in the extracellular space. We have demonstrated here that, if this localized concentration is high enough, cancer cells can be effectively killed without the requirement that they be internalized.

Intracellular Distribution of Nanoparticles. According to the cell uptake studies, the maximum uptake of nanoparticles should have been reached in 18 h. The confocal microscopy images below display the localization of the NPs, PCNP and PCNP-P which have been incubated with HT29 cells for 20 h and washed three times with media prior to imaging. The confocal images were captured at 633 nm (Figure 2), and 633 and 405 nm (Figure 3).

Although, the PC absorbs significantly at approximately 400 nm, excitation at 405 nm gave no fluorescence from the PCNP. Thus, the fluorescence observed with PCNP-P (excited at 405 nm) was considered to be only that emitted by porphyrin.

As can be seen from Figure 3, cells show granular fluorescence (PC and porphyrin), suggesting localization of the nanoparticles in endocytic vessels.[58]

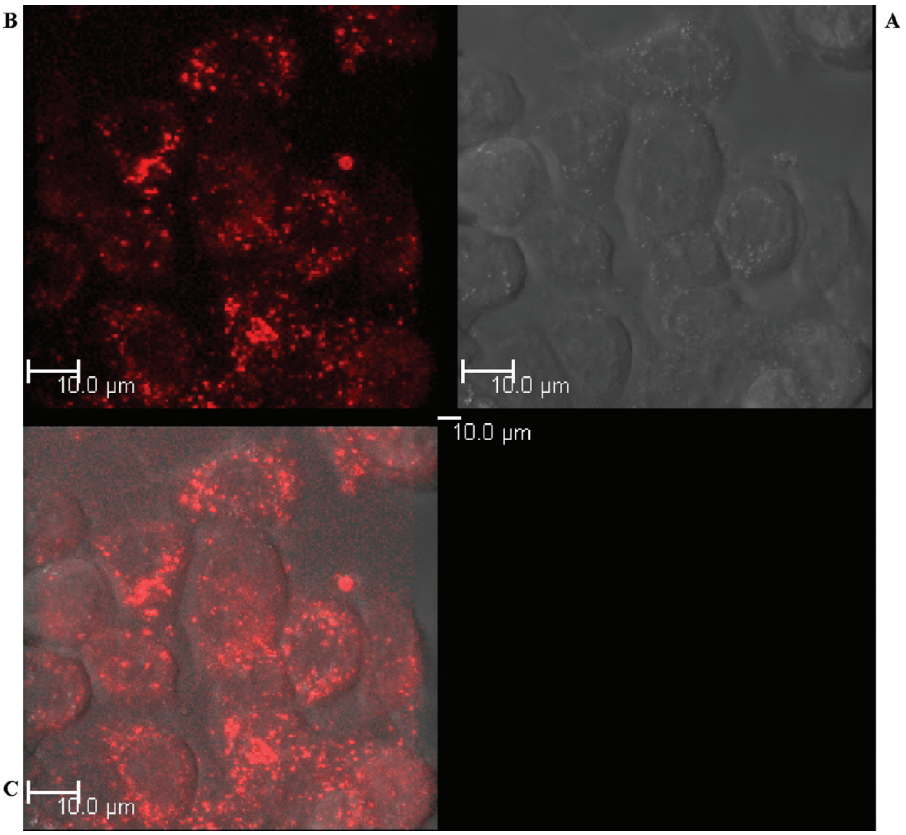

Figure 2. Confocal images of PCNP internalized in HT29 cells (after incubating for 20 h): (A) HT29 cells only, (B) PC emission, and (C) merged image.

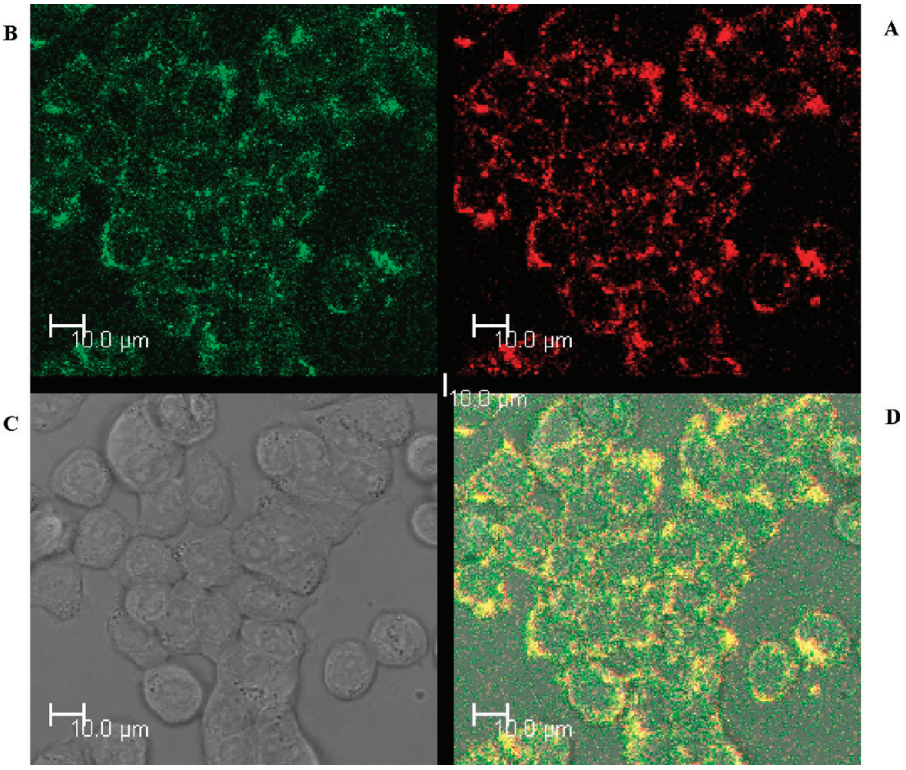

Figure 3. Confocal images (Leica) of PCNP-P internalized in HT29 cells (after incubating for 20 h) (red, excited at 633 nm; green, excited at 405 nm): (A) PC emission, (B) porphyrin emission, (C) HT29 cells only, and (D) merged image.

4. CONCLUSIONS

The results presented here indicate that polyacrylamide nanoparticles have potential as delivery vehicles for photodynamic agents in photodynamic therapy for cancer. Both internally trapped photosensitizers and analogues with a second photosensitizer conjugated to the particles after formation were active against HT-29 cells, but the latter was the more powerful PDT agent when the particles were internalized. The ability to deliver more than one class of photosensitizer could be advantageous clinically, as the larger spectral region covered could lead to more efficient absorption of light. The ability to deliver more than one class of photosensitizer could be advantageous clinically, as the larger spectral region covered could lead to more efficient absorption of light. The cationic nature of PCNP-P also makes it potentially attractive for photodynamic antimicrobial chemotherapy (PACT).

Results also show that cellular internalization is not necessary to photodynamically kill cancer cells, although internalized particles are also active; this could be important as *in vivo* significant amounts of nanoparticle would be expected to accumulate in the extracellular space in tumors due to the enhanced permeability and retention effect.

AUTHOR INFORMATION

Corresponding Author

*Department of Chemistry, University of Hull, Cottingham Road, Hull HU6 7RX, U.K. E-mail: r.w.boyle@hull.ac.uk. Tel: (01482) 466353. Fax: (01482) 466410.

ABBREVIATIONS

PDT, photodynamic therapy; PS, photosensitizer; NP, nanoparticles; PCS, photon correlation spectroscopy; TEM, transmission electron microscopy; FACS, fluorescence activated cell sorting; AlPc, aluminum phthalocyanine; PC, phthalocyanine; PCNP, polymer bound tetrasulfonato-aluminum phthalocyanine entrapped nanoparticles; PCNP-A, polymer bound amino functionalized tetrasulfonato-aluminum phthalocyanine entrapped nanoparticles; PCNP-P, polymer bound tetrasulfonato-aluminum phthalocyanine entrapped porphyrin conjugated nanoparticles; PBS, phosphate buffered saline; BSA, bovine serum albumin; NHS, 5-[4-(succinimide-N-oxycarbonyl)phenyl]-10,15,20-tris-(4- N-methylpyridimiumyl)porphyrin trichloride

REFERENCES

(1) Dolmans, D. E. J. G. J.; Fukumura, D.; Jain, R. K. Photodynamic therapy for cancer. *Nat. Rev. Cancer* **2003**, *3* (5), 380–387.

(2) Kübler, A. C. Photodynamic therapy. *Med. Laser Appl.* **2005**, *20* (1), 37–45.

(3) Josefsen, L. B.; Boyle, R. W. Photodynamic therapy: novel third-generation photosensitizers one step closer? *Br. J. Pharmacol.* **2008**, *154* (1), 1–3.

(4) Palumbo, G. Photodynamic therapy and cancer: a brief sightseeing tour. *Expert Opin. Drug Delivery* **2007**, *4* (2), 131–148.

(5) Hopper, C. Photodynamic therapy: a clinical reality in the treatment of cancer. *Lancet Oncol.* **2000**, *1*, 212–9.

(6) Dougherty, T. J.; Gomer, C. J.; Henderson, B. W.; Jori, G.; Kessel, D.; Korbelik, M.; Moan, J.; Peng, Q. Photodynamic therapy. *J. Natl. Cancer Inst.* **1998**, *90* (12), 889–905.

(7) Josefsen, L. B.; Boyle, R. W. Photodynamic therapy and the development of metal-based photosensitisers. *Met. Based Drugs* **2008**, *2008*, 276109.

(8) Wang, S. Z.; Gao, R. M.; Zhou, F. M.; Selke, M. Nanomaterials and singlet oxygen photosensitizers: potential applications in photodynamic therapy. *J. Mater. Chem.* **2004**, *14* (4), 487–493.

(9) Konan, Y. N.; Gurny, R.; Allemann, E. State of the art in the delivery of photosensitizers for photodynamic therapy. *J. Photochem. Photobiol., B* **2002**, *66* (2), 89–106.

(10) Bechet, D.; Couleaud, P.; Frochot, C.; Viriot, M. L.; Guillemin, F.; Barberi-Heyob, M. Nanoparticles as vehicles for delivery of photodynamic therapy agents. *Trends Biotechnol.* **2008**, *26* (11), 612–621.

(11) Cho, K. J.; Wang, X.; Nie, S. M.; Chen, Z.; Shin, D. M. Therapeutic nanoparticles for drug delivery in cancer. *Clin. Cancer Res.* **2008**, *14* (5), 1310–1316.

(12) Owens, D. E., III; Peppas, N. A. Opsonization, biodistribution, and pharmacokinetics of polymeric nanoparticles. *Int. J. Pharm.* **2006**, *307* (1), 93–102.

(13) Moghimi, S. M.; Hunter, A. C.; Murray, J. C. Nanomedicine: current status and future prospects. *FASEB J.* **2005**, *19* (3), 311–330.

(14) Poulsen, A. K.; Scharff-Poulsen, A. M.; Olsen, L. F. Horseradish peroxidase embedded in polyacrylamide nanoparticles enables optical detection of reactive oxygen species. *Anal. Biochem.* **2007**, *366* (1), 29–36.

(15) Gratton, S. E. A.; Ropp, P. A.; Pohlhaus, P. D.; Luft, J. C.; Madden, V. J.; Napier, M. E.; DeSimone, J. M. The effect of particle design on cellular internalization pathways. *Proc. Natl. Acad. Sci. U.S.A.* **2008**, *105* (33), 11613–11618.

(16) Zhang, L. W.; Monteiro-Riviere, N. A. Mechanisms of Quantum Dot Nanoparticle Cellular Uptake. *Toxicol. Sci.* **2009**, *110* (1), 138–155.

(17) Wartlick, H.; Spankuch-Schmitt, B.; Strebhardt, K.; Kreuter, J.; Langer, K. Tumour cell delivery of antisense oligonucleotides by human serum albumin nanoparticles. *J. Controlled Release* **2004**, *96* (3), 483–495.

(18) Hu, L.; Mao, Z. W.; Gao, C. Y. Colloidal particles for cellular uptake and delivery. *J. Mater. Chem.* **2009**, *19* (20), 3108–3115.

(19) Panyam, J.; Labhasetwar, V. Dynamics of endocytosis and exocytosis of poly(D,L-lactide-co-glycolide) nanoparticles in vascular smooth muscle cells. *Pharm. Res.* **2003**, *20* (2), 212–220.

(20) Besterman, J. M.; Low, R. B. Endocytosis - a Review of Mechanisms and Plasma-Membrane Dynamics. *Biochem. J.* **1983**, *210* (1), 1–13.

(21) Jin, H.; Heller, D. A.; Strano, M. S. Single-particle tracking of endocytosis and exocytosis of single-walled carbon nanotubes in NIH-3T3 cells. *Nano Lett.* **2008**, *8* (6), 1577–1585.

(22) Brannon-Peppas, L.; Blanchette, J. O. Nanoparticle and targeted systems for cancer therapy. *Adv. Drug Delivery Rev.* **2004**, *56* (11), 1649–1659.

(23) Oh, J. K.; Drumright, R.; Siegwart, D. J.; Matyjaszewski, K. The development of microgels/nanogels for drug delivery applications. *Prog. Polym. Sci.* **2008**, *33* (4), 448–477.

(24) Faraji, A. H.; Wipf, P. Nanoparticles in cellular drug delivery. *Bioorg. Med. Chem.* **2009**, *17* (8), 2950–2962.

(25) Brigger, I.; Dubernet, C.; Couvreur, P. Nanoparticles in cancer therapy and diagnosis. *Adv. Drug Delivery Rev.* **2002**, *54* (5), 631–651.

(26) Buck, S. M.; Koo, Y. E. L.; Park, E.; Xu, H.; Philbert, M. A.; Brasuel, M. A.; Kopelman, R. Optochemical nanosensor PEBBLEs: photonic explorers for bioanalysis with biologically localized embedding. *Curr. Opin. Chem. Biol.* **2004**, *8* (5), 540–546.

(27) Buck, S. M.; Xu, H.; Brasuel, M.; Philbert, M. A.; Kopelman, R. Nanoscale probes encapsulated by biologically localized embedding (PEBBLEs) for ion sensing and imaging in live cells. *Talanta* **2004**, *63* (1), 41–59.

(28) Almdal, K.; Sun, H. H.; Poulsen, A. K.; Arleth, L.; Jakobsen, I.; Gu, H.; Scharff-Poulsen, A. M. Fluorescent gel particles in the nanometer range for detection of metabolites in living cells. *Polym. Adv. Technol.* **2006**, *17* (9−10), 790–793.

(29) Tang, W.; Xu, H.; Park, E. J.; Philbert, M. A.; Kopelman, R. Encapsulation of methylene blue in polyacrylamide nanoparticle

platforms protects its photodynamic effectiveness. *Biochem. Biophys. Res. Commun.* **2008**, *369* (2), 579–583.

(30) Reddy, G. R.; Bhojani, M. S.; McConville, P.; Moody, J.; Moffat, B. A.; Hall, D. E.; Kim, G.; Koo, Y. E. L.; Woolliscroft, M. J.; Sugai, J. V.; Johnson, T. D.; Philbert, M. A.; Kopelman, R.; Rehemtulla, A.; Ross, B. D. Vascular targeted nanoparticles for imaging and treatment of brain tumors. *Clin. Cancer Res.* **2006**, *12* (22), 6677–6686.

(31) Kopelman, R.; Koo, Y. E. L.; Philbert, M.; Moffat, B. A.; Reddy, G. R.; McConville, P.; Hall, D. E.; Chenevert, T. L.; Bhojani, M. S.; Buck, S. M.; Rehemtulla, A.; Ross, B. D. Multifunctional nanoparticle platforms for in vivo MRI enhancement and photodynamic therapy of a rat brain cancer. *J. Magn. Magn. Mater.* **2005**, *293* (1), 404–410.

(32) Clark, H. A.; Hoyer, M.; Philbert, M. A.; Kopelman, R. Optical nanosensors for chemical analysis inside single living cells. 1. Fabrication, characterization, and methods for intracellular delivery of PEBBLE sensors. *Anal. Chem.* **1999**, *71* (21), 4831–4836.

(33) Sun, H.; Scharff-Poulsen, A. M.; Gu, H.; Almdal, K. Synthesis and Characterization of Ratiometric, pH Sensing Nanoparticles with Covalently Attached Fluorescent Dyes. *Chem. Mater.* **2006**, *18* (15), 3381–3384.

(34) Greish, K. Enhanced permeability and retention of macromolecular drugs in solid tumors: A royal gate for targeted anticancer nanomedicines. *J. Drug Targeting* **2007**, *15* (7−8), 457–464.

(35) Clark, H. A.; Hoyer, M.; Parus, S.; Philbert, M. A.; Kopelman, R. Optochemical Nanosensors and Subcellular Applications in Living Cells. *Microchim. Acta* **1999**, *131* (1), 121–128.

(36) Brasuel, M. G.; Miller, T. J.; Kopelman, R.; Philbert, M. A. Liquid polymer nano-PEBBLEs for Cl- analysis and biological applications. *Analyst* **2003**, *128* (10), 1262–1267.

(37) Clark, H. A.; Barker, S. L. R.; Brasuel, M.; Miller, M. T.; Monson, E.; Parus, S.; Shi, Z. Y.; Song, A.; Thorsrud, B.; Kopelman, R.; Ade, A.; Meixner, W.; Athey, B.; Hoyer, M.; Hill, D.; Lightle, R.; Philbert, M. A. Subcellular optochemical nanobiosensors: probes encapsulated by biologically localised embedding (PEBBLEs). *Sens. Actuators, B* **1998**, *51* (1−3), 12–16.

(38) Xu, H.; Aylott, J. W.; Kopelman, R.; Miller, T. J.; Philbert, M. A. A real-time ratiometric method for the determination of molecular oxygen inside living cells using sol-gel-based spherical optical nanosensors with applications to rat C6 glioma. *Anal. Chem.* **2001**, *73* (17), 4124–4133.

(39) Webster, A.; Compton, S. J.; Aylott, J. W. Optical calcium sensors: development of a generic method for their introduction to the cell using conjugated cell penetrating peptides. *Analyst* **2005**, *130* (2), 163–170.

(40) Conner, S. D.; Schmid, S. L. Regulated portals of entry into the cell. *Nature* **2003**, *422* (6927), 37–44.

(41) Rogers, W. J.; Basu, P. Factors regulating macrophage endocytosis of nanoparticles: implications for targeted magnetic resonance plaque imaging. *Atherosclerosis* **2005**, *178* (1), 67–73.

(42) Raynal, I.; Prigent, P.; Peyramaure, S.; Najid, A.; Rebuzzi, C.; Corot, C. Macrophage endocytosis of superparamagnetic iron oxide nanoparticles - Mechanisms and comparison of Ferumoxides and Ferumoxtran-10. *Invest. Radiol.* **2004**, *39* (1), 56–63.

(43) Josefsen, L. B; Aylott, J. W.; Beeby, A.; Warburton, P.; Boyle, J. P.; Peers, C.; Boyle, R. W. Porphyrin-nanosensor conjugates. New tools for the measurement of intracellular response to reactive oxygen species. *Photochem. Photobiol. Sci.* **2010**, *9*, 801–811.

(44) Kadish, K. M.; Smith, K. M.; Guilard, R.; *The Porphyrin Handbook - Synthesis and Organic Chemistry*; Academic Press: New York, 2000; Vol. 1.

(45) Tome, J. P. C.; Neves, M.; Tomes, A. C.; Cavaleiro, J. A. S.; Soncin, M.; Magaraggia, M.; Ferro, S.; Jori, G. Synthesis and antibacterial activity of new poly-S-lysine-porphyrin conjugates. *J. Med. Chem.* **2004**, *47* (26), 6649–6652.

(46) Valenzeno, D. P. *Advanced Study Institute on Photobiological, T. In Photobiological techniques: [proceedings of a NATO Advanced Study Institute on Photobiological Techniques, held July 1−4, 1990, in Kingston, Ontario, Canada]*; Plenum Press: New York, 1991.

(47) Osada, K.; Ravandi, A.; Kuksis, A. Rapid analysis of oxidized cholesterol derivatives by high-performance liquid chromatography combined with diode-array ultraviolet and evaporative laser light-scattering detection. *J. Am. Oil Chem. Soc.* **1999**, *76* (7), 863–871.

(48) Mosmann, T. Rapid colorimetric assay for cellular growth and survival: Application to proliferation and cytotoxicity assays. *J. Immunol. Methods* **1983**, *65* (1−2), 55–63.

(49) Roy, I.; Ohulchanskyy, T. Y.; Pudavar, H. E.; Bergey, E. J.; Oseroff, A. R.; Morgan, J.; Dougherty, T. J.; Prasad, P. N. Ceramic-based nanoparticles entrapping water-insoluble photosensitizing anticancer drugs: A novel drug-carrier system for photodynamic therapy. *J. Am. Chem. Soc.* **2003**, *125* (26), 7860–7865.

(50) Josefsen, L. B. Porphyrin-Nanosensor conjugates: novel tools for the study of cellular response to oxidative stress. Hull University, 2007.

(51) Kano, K.; Miyake, T.; Uomoto, K.; Sato, T.; Ogawa, T.; Hashimoto, S. Evidence for Stacking of Cationic Porphyrin in Aqueous-Solution. *Chem. Lett.* **1983**, *12*, 1867–1870.

(52) McAllister, K.; Sazani, P.; Adam, M.; Cho, M. J.; Rubinstein, M.; Samulski, R. J.; DeSimone, J. M. Polymeric Nanogels Produced via Inverse Microemulsion Polymerization as Potential Gene and Antisense Delivery Agents. *J. Am. Chem. Soc.* **2002**, *124* (51), 15198–15207.

(53) Bajpai, A. K.; Giri, A. Water sorption behaviour of highly swelling (carboxy methylcellulose-g-polyacrylamide) hydrogels and release of potassium nitrate as agrochemical. *Carbohydr. Polym.* **2003**, *53* (3), 271–279.

(54) Kim, J. S.; Yoon, T. J.; Yu, K. N.; Noh, M. S.; Woo, M.; Kim, B. G.; Lee, K. H.; Sohn, B. H.; Park, S. B.; Lee, J. K.; Cho, M. H. Cellular uptake of magnetic nanoparticle is mediated through energy-dependent endocytosis in A549 cells. *J. Vet. Sci.* **2006**, *7* (4), 321–326.

(55) Alberola, A. P.; Rädler, J. O. The defined presentation of nanoparticles to cells and their surface controlled uptake. *Biomaterials* **2009**, *30* (22), 3766–3770.

(56) Castilla, R.; Gonzalez, R.; Fouad, D.; Fraga, E.; Muntane, J. Dual effect of ethanol on cell death in primary culture of human and rat hepatocytes. *Alcohol Alcoholism* **2004**, *39* (4), 290–296.

(57) Wieder, M. E.; Hone, D. C.; Cook, M. J.; Handsley, M. M.; Gavrilovic, J.; Russell, D. A. Intracellular photodynamic therapy with photosensitizer-nanoparticle conjugates: cancer therapy using a 'Trojan horse'. *Photochem. Photobiol. Sci.* **2006**, *5* (8), 727–734.

(58) Selbo, P. K.; Hogset, A.; Prasmickaite, L.; Berg, K. Photochemical internalisation: A novel drug delivery system. *Tumor Biol.* **2002**, *23* (2), 103–112.